Determination of the electroporation onset of bilayer lipid membranes as a novel approach to establish ternary phase diagrams: example of the L-α-PC/SM/cholesterol system

Iris van Uitert, Séverine Le Gac* and Albert van den Berg

Received 30th March 2010, Accepted 10th June 2010
DOI: 10.1039/c0sm00181c

The lipid matrix of cell membranes contains phospholipids belonging to two main classes, glycero- and sphingolipids, as well as cholesterol. This matrix can exist in different phases, liquid disordered (l_d), liquid ordered (l_o) and possibly solid (s_o), or even a combination of these. The precise phase composition of a membrane depends on its molecular content and more specifically on the presence and amount of cholesterol. This in turn dictates the membrane properties. In this work, the resistance of membranes to the process of electroporation is studied and related to the membrane phase composition. Specifically, the threshold voltage for electroporation is measured (V_{th}) when DC pulses with increasing amplitude are applied to membranes prepared from various mixtures of a glycerolipid (Heart PC (L-α-PC)), a sphingolipid (Egg SM (SM)) and cholesterol (Ch), introduced in various ratios. Binary mixtures (L-α-PC/Ch, L-α-PC/SM, SM/Ch) and L-α-PC/SM/Ch ternary mixtures are successively employed. For all binary and ternary systems, dramatic changes in V_{th} are measured as a function of the membrane molecular composition, and the variation patterns of V_{th} are successfully correlated with the membrane phase composition. Interestingly, the measure of the electroporation onset can be employed as a novel methodology to establish ternary phase diagrams, and this is illustrated with the L-α-PC/SM/cholesterol ternary system.

Introduction

One of the main functions of a cell membrane is to act as an impermeable barrier to foreign entities such as genes, drugs or particles. For many applications, like DNA transfection or drug research, transporting foreign entities into a cell is crucial. This is achieved by transiently permeabilizing the cell membrane. A commonly used technique for this purpose is electroporation[1–3] which relies on the application of short pulses (μs and ms pulse length) of a high external electric field across a cell.[4,5] When the imposed transmembrane potential reaches a threshold value of about 0.2–1 V, a rearrangement in the molecular structure of the membrane occurs, leading to the creation of (transient) pores and a substantial increase in the cell's permeability. While this technique has been gaining in popularity for the last few decades (especially for cell transfection[6–8]) the overall success rate of the process remains low and still requires further optimization.[9]

One approach to increase the electroporation yield consists of getting a better understanding of the mechanism(s) of pore formation and of identifying key-parameters for this process through experimental work and/or theoretical modeling. Experimental studies have demonstrated that pores originate in the lipid matrix of the membrane.[10] Moreover, the time scale for their formation as well as their average size have been determined using both cells[10–12] and model membranes.[10,12–18] A model for the process of pore formation upon application of a potential across the membrane has been proposed using molecular dynamics simulations. This process includes three distinct steps:[17,19,20] (i) a local enhancement of the electric field and the creation of water defects, (ii) the formation of a water file through the membrane to create a hydrophobic pore and (iii) the rearrangement of the phospholipid molecules to create a hydrophilic pore.

Although these theoretical and experimental models have provided insight into the electroporation process, they present a major drawback in that they mostly approximate the membrane as a uniform phospholipid structure,[3,17,21] and only a few recent studies use more complex models such as binary phospholipid mixtures.[22,23] By contrast, the actual membrane of a cell is much more complex and this heterogeneity is known to affect its behavior and the resulting electroporation outcome.[21,24] For instance, Kanduser *et al.* showed that the cell membrane fluidity is a key-property of membranes for the process of pore formation,[24] and this is for a large part regulated by one specific component of cell membranes, cholesterol. The addition of cholesterol to phospholipid membranes changes their stability upon application of an electric field as a result of the specific interactions cholesterol establishes with the phospholipids.[21,25–31] Interestingly, the effect of cholesterol can be two-fold, depending on both the nature of the phospholipid molecules and the amount of cholesterol used. Furthermore, other components of cell membranes, peptides and proteins, also change the membranes' response to the applied electrical field by modifying the membrane properties locally.[32–34]

As mentioned, natural membranes are highly complex and they have first been described as a two-dimensional fluid with a considerable lateral homogeneity.[35,36] The basic structure and

BIOS, The Lab-on-a-Chip Group, MESA+ Institute for Nanotechnnology, University of Twente, Postbus 217, 7500AE Enschede, The Netherlands. E-mail: s.legac@utwente.nl; Fax: +31 (0)53 489 3595; Tel: +31 (0)53 489 2722

shape of such membranes are defined as a (phospho)lipid matrix which also serves as a substrate for membrane proteins.[36] This fluid mosaic model is dramatically simplifying the membrane structure with respect to the inhomogeneous distribution of the phospholipids and proteins; however, it still forms the basis for more recent and refined models.[37] Phospholipids are amphiphilic molecules that are composed of two main parts: (i) a hydrophilic head consisting of a backbone molecule, a phosphate and a polar group and (ii) two "parallel" hydrophobic chains of various lengths that can contain unsaturations. In natural membranes, two main types of phospholipids are found: glycero- and sphingolipids which have a glycerol or sphingosine backbone, respectively. The length of the hydrophobic chains and the amount of unsaturations together with the nature of the head group and the molecular shape of the phospholipids define the specific molecular properties of these phospholipids. These distinct properties particularly affect their packing pattern and density in membranes and consequently, the membrane fluidity and stability. At their melting temperature (T_m) which is specific for each phospholipid, phospholipids undergo a transition from the gel phase (L_β, also called the solid-ordered phase (s_o)), where the phospholipids chains are very ordered and the phospholipids can be tilted (indicated with a prime, L_β'), to a fluid phase (L_α, also named the liquid disordered phase (l_d)) when their chains melt and become disordered.[37] As suggested by the names of the phases, the phospholipids in the latter phase are less ordered than in the former one. This not only means that their diffusion rate in the plane of the membrane is higher but also that their *trans*/*gauche* ratio increases.[38] When cholesterol is present in the membranes, phospholipids are also found in a third phase, the liquid ordered phase (l_o).[39] The l_o phase is an intermediate phase between the two other phases; it combines the translational freedom found in the l_d phase together with the conformational order specific to the s_o phase.[38,40,41] Interestingly, the effect of cholesterol depends on the structural properties of the phospholipids. The two factors that determine the strength of cholesterol interactions with the phospholipids are the presence of unsaturations in the hydrocarbon chains and the nature of the backbone of the phospholipid. Cholesterol prefers saturated phospholipids having a sphingosine backbone.[38,39,42–46] Consequently, if the three components, glycero-, sphingolipids and cholesterol, are present in a membrane, phase separation occurs due to the fact that cholesterol preferably interacts with sphingolipids. The system undergoes a phase separation into a glycerolipid-rich l_d phase and sphingolipid- and cholesterol-rich (micro)domains of l_o phase. The size of the microdomain lies between 10 and 200 nm in cell membranes[47,48] while they have been reported to collide and coalesce in model systems to eventually give one large domain.[49,50] In the l_o domains, the lateral motion of phospholipid molecules is reduced and the membrane thickness increases due to the chain-straightening effect of cholesterol. l_o domains locally act as stiffening spots for the membranes, as is the case for the peptide gramicidin and the protein α-hemolysin.[31,32,34] Consequently, l_o domains should contribute to the stabilization of ternary model membranes containing cholesterol.

In our previous work, the influence of various cell membrane components on the electroporation process was investigated. There, the common synthetic phospholipid 1,2-diphytanoyl-*sn*-glycero-3-phosphocholine (DPhPC) was employed as a membrane basis where other phospholipids and cholesterol were successively added. The effect of the diversity in the membrane formulation on the resistance to pore formation in these model membranes was measured;[31] this has revealed that (i) the membrane composition is not to be neglected when studying the process of electroporation, and that (ii) the presence of cholesterol has a strong effect on the process of electroporation.

Our goal, in this article, is to examine further the role of cholesterol, and to better elucidate the mechanisms by which it changes the membrane properties and its resistance to the application of an external electric field. Cholesterol is an essential component of natural membranes. It can represent up to 30% of the membrane composition and is a key-element to regulate both the fluidity and the barrier properties of the cell membrane.[48,51,52] This well-known effect of cholesterol was observed in our previous experiments with a change in the membrane stability in a concentration-dependent manner.[31] However, a simplified system was employed, consisting of a membrane made from only one artificial glycerolipid (DPhPC). DPhPC belongs to the family of phospholipids that is abundantly found in the membranes of archeabacteria, organisms that can resist harsh conditions but whose membranes lack cholesterol. DPhPC molecules form tight networks due to the intertwining of their methylated hydrocarbon chains. DPhPC already condenses the membrane, as would cholesterol do in membranes based on phosphatidylcholines (PCs) which are mostly used for membrane experimentation. Moreover, due to the presence of a mixture of glycerolipids and sphingolipids in natural membranes, cholesterol can give rise to phase separation phenomena.[25] This possible phase separation and its effect on the membrane structure were neglected in our first study as SM was not included. Here, the aim is to reproduce better the complexity found in cell membranes and to study how this would affect the membrane resistance to electroporation. The measured trends in the threshold voltage for electroporation are correlated to (i) the presence of different phases (l_d, l_o or s_o) as a function of the membrane composition and (ii) the resulting phase separation phenomena (*i.e.* the co-existence of different phases) induced by cholesterol. For that purpose, ternary systems composed of glycerolipids (Heart PC, a mixture whose predominant species is 16:0/18:2 PC (named as L-α-PC in the rest of the article)), sphingolipids (Egg SM, a mixture whose predominant species is 16:0 SM (named as SM in the rest of the article)) and cholesterol, in which phase separation phenomena are expected to occur, are utilized. The employed phospholipids are natural mixtures and not purely synthetic phospholipids since the interest of this work lies in studying a system that comes as close as possible to the phospholipid composition found in cell membranes (where over a thousand different phospholipids are found[37]). Our approach consists of looking at the resistance of bilayer lipid membranes (BLMs) to an applied electric field, by increasing stepwise the amplitude of a DC signal applied on the membrane. Firstly, binary systems, L-α-PC/cholesterol, L-α-PC/SM and SM/cholesterol, are studied to elucidate individual interactions taking place between two molecular species. Following this, ternary systems are investigated to understand how interactions between the three components affect the membrane resistance to electroporation and which parameters are the most important in this.

Interestingly, these results enable us to propose a ternary phase diagram for the L-α-PC/SM/cholesterol system derived from the measured electroporation results of the binary and ternary systems.

Materials and methods

Chemicals

Lipids (Heart PC, a mixture whose predominant species is 16:0/18:2 PC (L-α-PC), Egg SM, a mixture whose predominant species is 16:0 SM (SM), and cholesterol (Ch) (Fig. 1)) are purchased from Avanti Polar Lipids (Alabaster, AL). KCl, *n*-decane and chloroform are purchased from Sigma-Aldrich (St Louis, MO). Hepes is purchased from Merck Chemicals (Darmstadt, Germany). Deionized water (18.2 MΩ × cm) which is used for all solution preparation and cleaning procedures is obtained using a MilliQ system (Millipore, Billerica, MA).

Measurement set-up

A conventional bilayer system (Warner Instruments, Hamden, CT) is used for BLM experimentation. This system comprises of a Delrin cup and chamber containing two round compartments. The cup is inserted in the *trans*-compartment of the chamber, and the compartments are connected *via* a 150 μm aperture in the cup across which BLMs are prepared. Both compartments contain 1 mL buffer solution (10 mM Hepes, 1 M KCl, pH 7.4) and Ag/AgCl electrodes (used for the electrical characterization of the BLMs). Electrical measurements are carried out with an Axopatch 200b amplifier (Molecular devices, Sunnyvale, CA), applying voltages and measuring currents across the bilayer. Data-acquisition is performed with LabVIEW and a PCI-6259 data acquisition card (National Instruments, Austin, TX). All measurements are performed at room temperature.

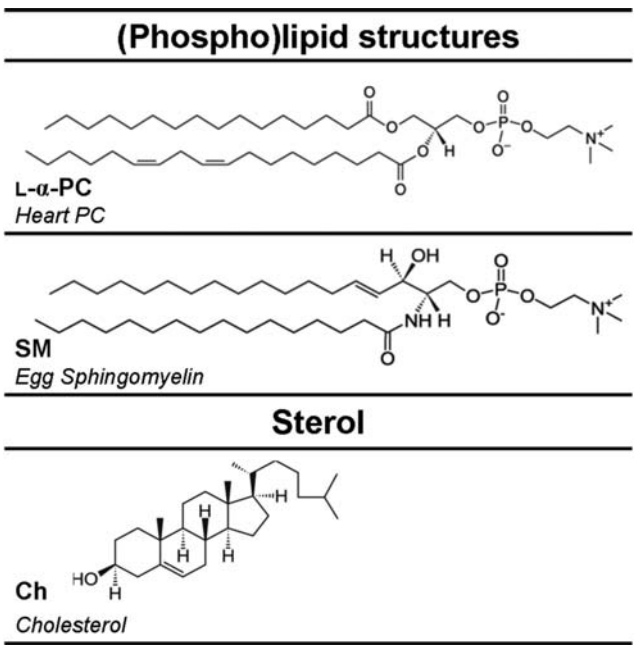

Fig. 1 Molecular structures of L-α-phosphatidylcholine (L-α-PC), sphingomyelin (SM), and cholesterol (Ch) used in this study. For L-α-PC and SM, the structure of the predominant species found in the mixtures are indicated.

Preparation and characterization of BLMs

All lipids are used as chloroform-based solutions. All phospholipids are purchased at 10 mg mL^{-1} solutions in chloroform, and cholesterol as a powder and dissolved in chloroform to yield a 25 mg mL^{-1} solution. Before the preparation of BLMs, a few tenths of μL of the lipid solution in chloroform is left to evaporate overnight, yielding an amount of 250 μg dried lipids, and subsequently dissolved in *n*-decane at a final concentration of 25 mg mL^{-1}. To improve the solubility of sphingomyelin and cholesterol 2–3% ethanol can be added. The resulting *n*-decane solutions are used for the preparation of BLMs.

Bilayer lipid membranes are created using the Mueller–Rudin technique.[53] Bilayer formation is monitored using the Axopatch amplifier and characterized by a drop in the current due to the GΩ seal between the bilayer and the aperture. Thereafter, the membrane capacitance is measured as previously described to confirm the formation of a BLM.[54]

Determination of the electroporation threshold of BLMs

The electroporation threshold (V_{th}) of the membrane is defined as the voltage at which the membrane conductivity increases due to the creation of pore(s). This value is determined as the value at which a leakage current is measured through the membrane. For that purpose, a DC voltage is applied to the membrane using the Axopatch amplifier and gradually increased (every 30 s) by steps of 20 mV until peaks larger than three times the root mean-square of the noise are observed in the measured current. Pore formation is checked by re-applying the voltage at which peaks are detected; this confirms that the peaks are not due to imperfections in the membrane. The voltage value found corresponds to the electroporation threshold V_{th}. For every membrane composition, V_{th} is determined at least three independent times and the indicated value corresponds to the average of the separate measurements.

Results and discussion

The aim of this work is to correlate the resistance of model membranes to the application of an electric field with its composition to get a better understanding of processes involved in the technique of electroporation. For that purpose, ternary mixtures of high T_m sphingolipids (Egg SM, SM), low T_m glycerolipids (heart PC, L-α-PC), and cholesterol are employed. These are three key-components of the lipid matrix of cell membranes which are well-known to influence the membrane properties and phase composition. However, in order to be able to comprehend fully the intricate molecular interactions occurring in ternary systems, interactions taking place between different components in the individual binary systems must firstly be characterized.

Binary systems

In the coming section, three different binary systems are considered composed of natural phospholipids: (i) L-α-PC/cholesterol, (ii) SM/cholesterol and (iii) L-α-PC/SM.

L-α-PC/cholesterol. As shown in Fig. 2, the variations of V_{th} for L-α-PC membranes containing 0–60% cholesterol can be divided in four (concentration-dependent) domains that are indicated by dashed lines in the graph. At low cholesterol concentrations, a progressive decrease in V_{th} from 165 ± 19 mV for 0% cholesterol to 112 ± 30 mV for 21% cholesterol is observed. In the next section, V_{th} rises slowly up to 200 ± 37 mV upon addition of cholesterol (until 33% Ch). In the third section of the plot, a steeper variation of V_{th} that reaches the value of 420 ± 35 mV for 39.5% cholesterol is seen. Finally, above 39.5% cholesterol, there is no further change in V_{th}, and a plateau is observed.

Interactions taking place between L-α-PC and cholesterol are responsible for these multiple variations in V_{th} as cholesterol can induce phase transitions in L-α-PC/cholesterol mixtures in a concentration-dependent manner. From the literature it is known that a phospholipid having a low T_m undergoes one phase transition, notably upon addition of cholesterol; from the l_d phase (<∼20% cholesterol) to a pure l_o phase at high cholesterol concentrations (>∼50% cholesterol). This transition and the phase behavior of a phospholipid depend on its T_m.[55] Between these two well-defined phases, an intermediate regime is found where the l_d and l_o phases coexist.[55] The employed glycerolipid, L-α-PC is harvested from natural cell membranes and contains a mixture of different types of glycerolipids so that its transition temperature is hard to pin-point. Nevertheless, its value can be estimated by looking at the transition temperature reported for the glycerolipid that is the most predominant in the mixture. The most abundant species in the mixture is asymmetric with one saturated tail of 16 carbons (16:0) and one double unsaturated tail of 18 carbons (18:2). 16:0/18:2 PCs are reported to have a T_m below −16 °C,[56] so that L-α-PC membranes are in the l_d phase at room temperature. Although the phospholipids are mobile in this phase, they cannot pack very densely due to kinking of the tails containing unsaturations.[51] Another consequence of the presence of an unsaturated chain is that L-α-PC is likely not to interact with cholesterol, as such an interaction is thermodynamically disfavored.[25] Therefore, at low concentrations (<20% Ch) there is no positive interaction between cholesterol and L-α-PC, and the amount of defects in the membrane is increased due to the negative intrinsic monolayer curvature of cholesterol.[43,57–59] As the membrane stability directly correlates with the phospholipid packing density, the addition of cholesterol till 20% facilitates the process of (electro)pore formation. On the contrary, at higher concentrations, cholesterol promotes the ordering of the hydrocarbon chains of the phospholipids.[25,26,30] Furthermore, cholesterol binds the phospholipids together in order to shield itself from the aqueous solution around the membrane, as it does not like to interact with water.[26,60] The combination of both the chain ordering and the condensing effects results in a local densification of the phospholipids in the membrane around the molecules of cholesterol. Therefore, the phospholipids that bind to cholesterol are in the l_o phase. In that phase, phospholipids are more ordered, packed more tightly and have a relatively high mobility (although lower than in the l_d phase).[38,61] In turn, the membrane thickens and better resists the application of an electric field as observed for cholesterol amounts of 20–33%. Nevertheless, this increase in V_{th} is limited as the fraction of the phospholipids in the l_d phase still surpasses that in the l_o phase. When the cholesterol amount exceeds 33%, V_{th} increases steeply; the fraction of the phospholipids in the l_o phase surpasses that of the l_d phase, and the strengthening effect of the l_o phase is dominant. Furthermore, as the l_o domains grow in size but reduce in number due to their coalescence, the amount of packing defects at the interface of the two types of domains becomes smaller, which further disfavors pore formation. This upward trend in V_{th} would be expected to continue for larger cholesterol contents, but instead V_{th} levels off above 40% cholesterol. This plateau is to be accounted for by the maximum solubility of cholesterol in the membrane. The maximum solubility is reported to lie between 50% and 66%, depending on the phospholipid used.[60,62] Nevertheless, as cholesterol is reported to dislike interactions with phospholipids containing unsaturated tails such as L-α-PC,[44] it might already be expelled from the membrane at an even lower concentration than 50%. The measured plateau can reflect this, as the bilayer properties are not changed any further for cholesterol amounts above 50%. Membranes prepared with more than 60% of cholesterol are quickly destabilized, which confirms that cholesterol crystallizes and is expelled out of the membranes.

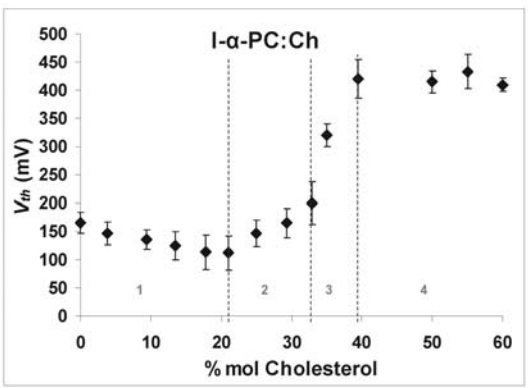

Fig. 2 Electroporation threshold V_{th} measured for the binary BLMs containing L-α-PC and cholesterol, plotted as a function of the cholesterol content. Vertical dashed lines depict the transitions between the different domains we distinguish (see text for more information).

SM/cholesterol. Following this, SM/cholesterol systems with cholesterol concentrations ranging from 35 to 60% were studied. Firstly, the transition temperature for natural SM, like the species used in this study, is reported to lie between 37°C and 48°C.[39] The purely SM membranes are subsequently in the solid phase at room temperature, and SM membranes with a cholesterol amount lower than 35% cannot be prepared at that temperature. Secondly, as already discussed for L-α-PC systems, 60% cholesterol is the upper limit for cholesterol solubility and no attempt was made to make membranes beyond this cholesterol amount.

As illustrated in Fig. 3, V_{th} exhibits a two-step increase as a function of the cholesterol content, from 40 ± 0 mV for

membranes containing 35% cholesterol to 207 ± 12 mV for 45% cholesterol, and up to 360 ± 0 mV for 60% cholesterol. From the literature it is known that SM membranes undergo a transition from the s_o phase to the l_o phase for an increasing cholesterol amount.[55] It is not possible to measure the s_o phase transition here, as those membranes cannot be prepared. However, their transition to the l_o phase is reported for around 25–30% cholesterol.[38,63] Consequently, in the first section of the curve (35–45% cholesterol), the membrane contains both s_o and l_o phases. In the s_o phase, the fluidity of the membrane is much lower than in the other phase. The voltage required to electroporate membranes is known to be lower for less fluid membranes,[24] and pores do not close easily when lipids move slowly.[21] Furthermore, the structural defects are the largest at the edge between the s_o and the l_o domains due to the phospholipid mismatch and pore formation should initiate at this interface. The progressive addition of cholesterol to such membranes not only disrupts the dense s_o phospholipid network and promotes the conversion into the l_o phase but also reduces the amount of phospholipid mismatch between the different domains. The membrane becomes more fluid and smoother, and this correlates with a linear increase in the membrane resistance to the applied electric field between 35 and 45% cholesterol. For a cholesterol amount higher than 45%, the membrane is again reported to be completely in the l_o phase.[55] The phospholipids are more organized in the same manner as observed for L-α-PC–cholesterol membranes (>40% Ch). The increase observed in the second section of the plot directly correlates to the transition of the membrane to the l_o phase, which is accompanied by its thickening.

L-α-PC/SM. Finally, L-α-PC/SM binary systems are investigated, and variations in the electroporation threshold for SM amounts from 0 to 66% are shown in Fig. 4. As mentioned previously, SM is in the solid phase at room temperature, and this prevents from preparing membranes with more than 66% SM. A continuous decrease of the electroporation threshold voltage V_{th} is observed as a function of the addition of SM, with still two different trends. In a first stage, V_{th} decreases linearly (165 ± 19 mV for 0% SM to 107 ± 12 mV for 40% SM) and

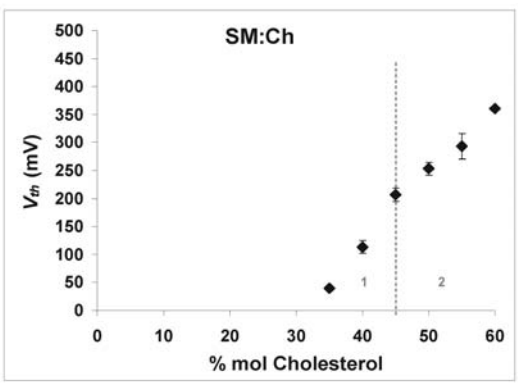

Fig. 3 Electroporation threshold V_{th} measured for the binary BLMs containing SM and cholesterol, plotted as a function of the cholesterol content. Vertical dashed lines depict the transitions between the different domains we distinguish (see text for more information).

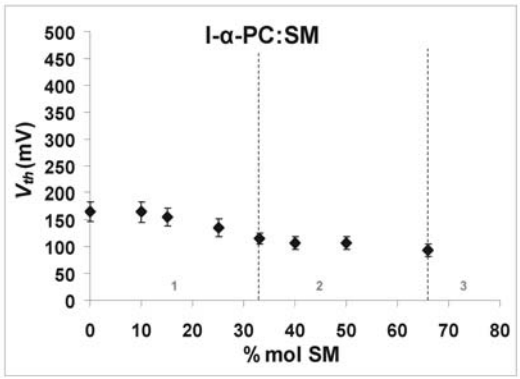

Fig. 4 Electroporation threshold V_{th} measured for the binary BLMs containing L-α-PC and SM, plotted as a function of the SM content. Vertical dashed lines depict the transitions between the different domains we distinguish (see text for more information).

subsequently levels off up to 66% SM (down to 93 ± 11 mV). Although the change in the slopes is subtle, this two-fold variation correlates again with two successive phase transitions reported for L-α-PC/SM systems (around 30% SM and 65% SM, respectively),[55] from the l_d phase *via* the co-existing l_d and s_o phases, to a pure s_o phase. Around 40% SM, s_o domains appear in the l_d matrix. These domains at first do not destabilize the membrane any further (second zone): the destabilizing properties of enlarging s_o domains are likely to be counterbalanced by a reduction of the destabilizing L-α-PC/SM contacts due to the s_o domain formation (creation of packing defects). In the last section of the curve (>66% SM), the s_o phase becomes most predominant, preventing stable membrane preparation.

Ternary systems of glycerolipids, sphingolipids and cholesterol

In the previous section, the individual basic binary interactions occurring between the three lipids, L-α-PC, SM and cholesterol, are examined. In the current section, this knowledge is applied to understand interactions found in ternary systems. Not only the precise molecular interactions in such a complex system are of interest, but also how the phase composition of the membrane influences the pore formation process. To study this, cholesterol is added to various binary L-α-PC/SM systems, and three examples of the V_{th} variations measured as a function of the amount of cholesterol are shown in Fig. 5, for ternary systems with a 2:1, a 1:1 and a 1:2 L-α-PC/SM molar ratio (Fig. 5a, b and c, respectively). All graphs present four regions characterized by different regimes in V_{th} variations (qualitative boundaries are again represented by dashed lines in the plots), as summarized in Table 1. In all three graphs, V_{th} exhibits a small decrease in the first zone, followed by a rise (second zone) and a plateau (third zone), and finally a second (steep) increase (fourth zone); the precise boundaries for the four zones in indicated in Table 1.

As for the binary systems, the different zones in the three graphs correlate to the different phases the phospholipids would be in according to the literature.[45,55,64] When all three components are mixed, the lipids separate in distinct phases, a glycerolipid-rich and cholesterol-depleted l_d phase and a sphingolipid-rich and cholesterol-rich l_o phase in

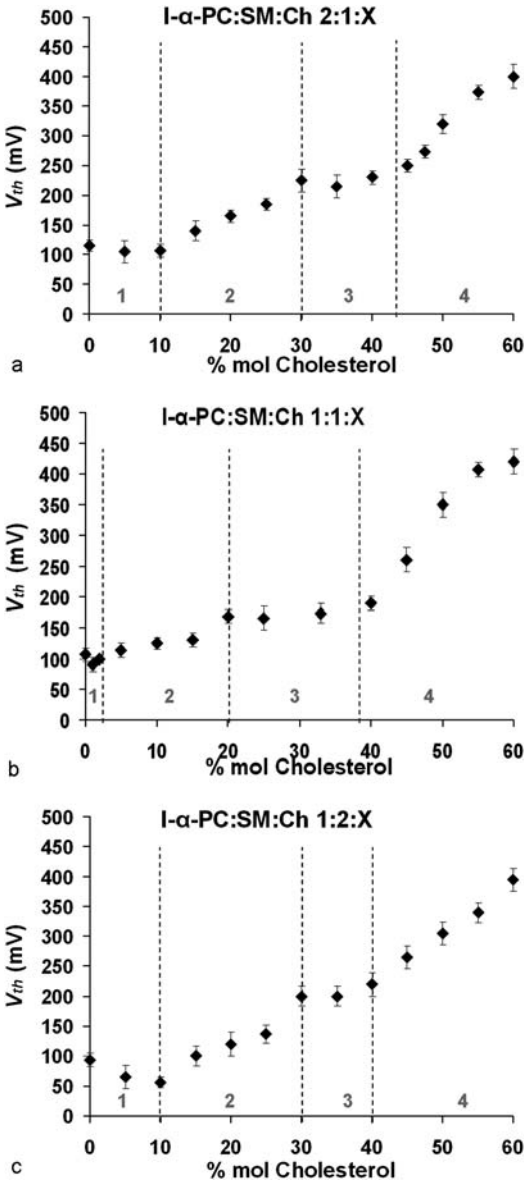

Fig. 5 Electroporation threshold V_{th} measured for BLMs made from a ternary mix of (a) 2:1 L-α-PC/SM and (b) 1:1 L-α-PC/SM (c) 1:2 L-α-PC/SM with increasing amounts of cholesterol, plotted as a function of the cholesterol content. Vertical dashed lines depict the transitions between the different domains we distinguish and the gray numbers in each domain refers to the different zones (see text for more information).

membranes.[25,38,39,45,48,55,61,63,64] Consequently, both phase transition and phase separation phenomena are expected to occur upon addition of cholesterol in the membranes. Interestingly, the different regions in our graphs (see Fig. 5 and Table 1) coincide with the phase domains reported for similar systems.[45,55,64] Table 1 summarizes the trends found in V_{th} together with the phenomena observed in the membrane in terms of phase composition and structure changes. Briefly, for all three systems, a progressive transition is observed from a l_d (2:1 L-α-PC/SM system) or a mixed $l_d - s_o$ phase (1:1 and 1:2 L-α-PC/SM systems) into a full l_o membrane,[55] with intermediary states with a coexisting (i) l_d and l_o phases (2:1 L-α-PC/SM system) or (ii) l_d, l_o, and s_o (1:1 and 1:2 L-α-PC/SM systems). The variations in the different zones are detailed below.

Zone 1 (l_d and $l_d - s_o$ phase). In this first zone, V_{th} progressively decreases for all three systems; the higher the amount of SM, the steeper the decrease. However, this variation is not accounted for by a phase transition but is linked to the precise molecular interactions in the membrane upon addition of cholesterol. The behavior of the first system is comparable to a membrane prepared from L-α-PC only (see Fig. 2): cholesterol is inserted between the phospholipids but does not develop any positive interactions with them. As before, the packing density of the phospholipid molecules is reduced, and pore formation becomes easier. For the two other systems, the situation is more complex as SM is in very tightly packed s_o domains, and most probably tilted.[65] Consequently, cholesterol accommodates itself first into l_d L-α-PC domains, as for the former system. However, part of the cholesterol still interacts with the s_o domains where SM molecules become untilted while remaining in the s_o phase. As before, the phospholipids are less densely packed, as reflected by the reduction measured in V_{th}. Interestingly, as the content in SM in the membrane is greater, the decline in V_{th} is more marked. This is related to the presence of more and larger s_o domains: not only the membrane becomes stiffer,[24] but the amount of packing defects between the domains is higher.

As a conclusion, for the three systems, the addition of a limited amount of cholesterol translates into the creation of packing defects in the membrane, which is in turn less resistant to the application of an electric field.

Zones 2–3 ($l_d - l_o$ and $l_d - l_o - s_o$ co-existing phases). In the two following zones (zone 2–3), V_{th} displays a two-step variation upon increasing cholesterol content: it first rises (zone 2) and subsequently gives a plateau (zone 3). As before, although the trends are similar for all three graphs, the precise phenomena responsible for these variations differ for the three graphs, as detailed in Table 1. The addition of cholesterol in membranes that are initially fully in the l_d phase (2:1 L-α-PC/SM ratio) triggers the successive phase transition of SM (zone 2) and PC (zone 2–3) into the l_o phase.[55] From the binary mixtures (see Fig. 3) we know that SM/Ch membranes are fully l_o when the SM/Ch ratio reaches 11:9. At the border between zones 2 and 3, the composition of the membrane is 23% SM, 47% L-α-PC and 30% cholesterol; the transformation of SM into l_o domains costs 20.5% of the 30% cholesterol. The remaining amount of cholesterol is subsequently employed to partially convert L-α-PC into the l_o phase. Subsequently, only in the third zone of the graph, l_d L-α-PC domains completely disappears into L-α-PC l_o domains. However, V_{th} exhibits a plateau in the zone 3, and not an increase as would be expected from the full conversion of the membrane into the l_o phase, revealing the existence of a counterbalancing effect. The growth of L-α-PC l_o domains is accompanied by the creation of more packing defects at the border between L-α-PC and SM l_o domains due to an increase in line tension and a difference in both the packing density[48,50,65] and domains thickness. This effect is negligible in the second zone as L-α-PC is distributed between the l_d and l_o phases and the amount of L-α-PC l_o domains remains small. The creation of additional packing defects is the counteracting force, accounting for the plateau found in V_{th}.

Table 1 Summary of the phenomena observed for the BLM electroporation experiments for the three L-α-PC/SM/cholesterol ternary systems having a 2:1, 1:1 and 1:2 L-α-PC:SM molar ratio and presented in Fig. 5: Borders of the 4 zones where the variation of V_{th} is monotonous, sense of V_{th} variations, phase composition of the membrane and major changes occurring in both the phase composition and the structure of the membrane.

	Zone (details)	2:1 PC:SM	1:1 PC:SM	1:2 PC:SM
1	Borders	0 → 10% cholesterol	0 → 2% cholesterol	0 → 10% cholesterol
	V_{th} variation	⇓	⇓	⇓
	Phase composition	l_d (SM; L-α-PC)	s_o (SM) l_d (L-α-PC)	s_o (SM) l_d (L-α-PC)
	Changes (Phase; Structure)	— [a] Packing defect creation [b]	— [a] Packing defect creation [b]	— [a] Packing defect creation [b]
2	Borders	10 → 30% cholesterol	2 → 20% cholesterol	10 → 30% cholesterol
	V_{th} variation	⇑	⇑	⇑
	Phase composition	$l_d + l_o$ (SM; L-α-PC)	$s_o + l_o$ (SM) $l_d + l_o$ (L-α-PC)	$s_o + l_o$ (SM) $l_d + l_o$ (L-α-PC)
	Changes (Phase; Structure)	SM: $l_d \rightarrow l_o$ L-α-PC: $l_d \rightarrow l_o$ ⇑ Thickness [c] ⇑ Packing density [c]	SM: $s_o \rightarrow l_o$ L-α-PC: $l_d \rightarrow l_o$ ⇑ Thickness [c] ⇑ Packing density [c]	SM: $s_o \rightarrow l_o$ ⇑ Thickness [c] ⇑ Packing density [c]
3	Borders	30 → 42% cholesterol	20 → 38% cholesterol	30 → 42% cholesterol
	V_{th} variation	Plateau	Plateau	Plateau
	Phase composition	l_o (SM) $l_d + l_o$ (L-α-PC)	l_o (SM) $l_d + l_o$ (L-α-PC)	l_o (SM) $l_d + l_o$ (L-α-PC)
	Changes (Phase; Structure)	L-α-PC: $l_d \rightarrow l_o$ ⇑ Thickness [c] ⇑ Packing density [c] ⇑ Packing defect creation [b]	L-α-PC: $l_d \rightarrow l_o$ ⇑ Thickness [c] ⇑ Packing density [c] ⇑ Packing defect creation [b]	L-α-PC: $l_d \rightarrow l_o$ ⇑ Thickness [c] ⇑ Packing density [c] ⇑ Packing defect creation [b]
4	Borders	42 → 60% cholesterol	38 → 60% cholesterol	42 → 60% cholesterol
	V_{th} variation	⇑⇑	⇑⇑	⇑⇑
	Phase composition	l_o (SM; L-α-PC)	l_o (SM; L-α-PC)	l_o (SM; L-α-PC)
	Changes (Phase; Structure)	— [a] ⇑ Thickness [c] ⇑ Packing density [c]	— [a] ⇑ Thickness [c] ⇑ Packing density [c]	— [a] ⇑ Thickness [c] ⇑ Packing density [c]

[a] No phase change. [b] Destabilizing effect. [c] Stabilizing effect.

The 1:1 and 1:2 L-α-PC/SM ratio membranes are in an intermixed $l_d - s_o$ phase at low cholesterol concentrations (5% and 10% respectively). Upon addition of cholesterol SM is again first converted into l_o domains, and the three phases co-exist (zone 2 in the graphs). The transformation of the SM s_o domains into l_o domains thickens the membrane and strengthens its resistance against pore formation, as reflected by the increase in V_{th}. In this zone, L-α-PC molecules are unaffected and remain in the l_d phase. For higher cholesterol contents (border between zone 2 and zone 3), all s_o domains have disappeared and the membrane is found in an intermixed $l_d - l_o$ phase. This $l_d - l_o$ region exhibits the same behavior as the 2:1 L-α-PC/SM systems, and the two same counteracting effects are found, giving rise to a plateau of V_{th}.

Zone 4 (l_o phase). For the highest cholesterol contents (fourth zone), all membranes are in a pure l_o phase;[45,55,64] they are consequently the most resistant to pore formation. As SM and L-α-PC give different packing pattern in the l_o phase, they form separated domains. The large V_{th} values in this last zone correlate to the denser phospholipid packing in both l_o domains upon further addition of cholesterol. Interestingly, the maximum value measured for V_{th} for l_o membranes phase is slightly lower for membranes containing higher amounts of SM. SM l_o domains are thinner than their counterparts formed from L-α-PC. Consequently, the average thickness of the membrane decreases for larger contents in SM, and this is directly reflected in the behavior of V_{th}.

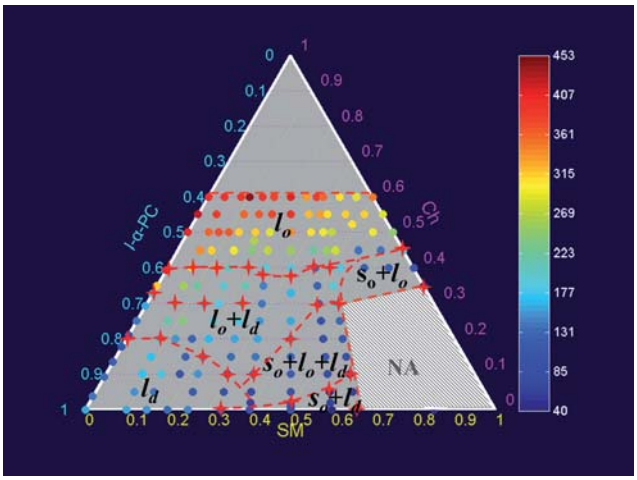

Fig. 6 Ternary graph derived using a novel technique: determining the membrane resistance to electroporation. The dots indicate individual values of electroporation threshold V_{th} in mV for various ternary mixtures made from L-α-PC, SM and cholesterol. The red stars indicate the phase transition boundaries for the discussed mixture and dashed lines possible phase boundaries.

Proposed L-α-PC/SM/cholesterol ternary phase diagram. As the trends found in the variations of V_{th} could be correlated with the phase composition of the membrane, and as they were in good agreement with other data reported in the literature,[55] the same measurements were subsequently carried out for other L-α-PC/SM/cholesterol ternary mixtures, in an attempt to derive a full ternary phase diagram for this L-α-PC/SM/cholesterol system. Fig. 6 depicts the resulting ternary diagram. First, the region at the top (>60% Ch) and the striped region at the right bottom corner of the graph (>66% SM and <40% Ch) correspond, respectively, to the region that is unavailable for measurements due to the large amount of cholesterol, and to the region where the s_o phase dominates, and this prevents the preparation of stable membranes, as mentioned earlier. For every region, the membrane phase composition can successfully be identified from the V_{th} variation pattern as before, and the resulting full diagram reasonably correlates to other ternary phase diagrams.[45,55,64,66] However, one region in the diagram still remains elusive; it corresponds to the so-called "three-phase-triangle", where all three phases (l_o, l_d and s_o) co-exist.[50,55] In this region, V_{th} remains relatively stable between 60 and 130 mV, compared to the variations observed in pure l_d and intermixed $l_d - s_o$ domains. As discussed already, this is caused by two counteracting effects: the growth of l_o domains and the apparition of additional packing defects due to a phospholipid mismatch at the domain border.

The full diagram clearly shows that the membrane composition strongly influences V_{th}, and the steepest variations are found for high cholesterol concentrations (>40%) where small changes in the membrane composition translate into dramatic alterations in V_{th}. Interestingly, the composition of natural cell membranes is found in this area: this indicates that small changes in the lipidic composition of a cell membrane would have a large effect on its response to the application of an electric field and on the outcome of the electroporation process. Moreover, the plasma membrane composition not only differs per cell type, but also per individual cell in the same culture or even locally in the cell membrane. As a consequence, each cell, and even different parts of the membrane, would respond differently to an applied electric field, explaining why the outcome of electroporation experiments varies so much for every cell. Consequently, the size of the cell is not the only factor to be taken into account when designing an electroporation protocol.

Differences between our diagram and previously reported diagrams. The precise phase boundaries defined by the variation trends of V_{th} do not fully correspond to those reported in the literature.[45,55,64] A first reason for this is that the PC species used here is different from those employed in those other studies (palmitoyloleoylphosphatidylcholine (POPC)[45,55,64] or dioleoylphosphatidylcholine (DOPC).[45] Secondly, L-α-PC and SM employed here are obtained from natural cell membranes: consequently, they are mixtures of several species, and not pure phospholipids as is the case in the other reports, and they contain impurities. The latter are known to have a dramatic effect on the overall behavior of the membrane.[50] On other aspects, the phase diagrams described in the literature have been obtained using a combination of other techniques, such as nuclear magnetic resonance (NMR),[67–69] electron spin resonance (ESR),[70] fluorescence microscopy,[45,55,68,71] differential scanning calorimetry (DSC)[64] and atomic force microscopy (AFM)[72–74] while here only electrical measurements are utilized. The technique employed to establish the diagram is also of influence on the precisely found borders between the regions in the diagram. Moreover, some of the aforementioned techniques require the addition of probes or the use of modified phospholipids, and this is notably the case for fluorescence measurements. Obviously, the presence of these probes affects the phospholipid packing density and changes the membrane phase behavior.[45] All these factors account for any difference found between these data and other data reported in literature.

Conclusion

Electroporation threshold for complex membrane mixtures

Most electroporation studies reported in the literature have been performed with only one type of phospholipid in the membrane, neglecting thereby the diversity found in natural cell membranes. Therefore, membranes combining natural glycero- and sphingolipids as well as cholesterol are employed here. Such models better represent what is happening in natural membranes when their composition is varied (either artificially, or between cells, or by the cell itself).

These model membranes give great variations in the threshold voltage for electroporation as a function of the membrane composition, which supports our approach. Interestingly, in the region where a cell membrane would fall in, slight changes in the composition have a large effect on its stability and the outcome of the electroporation process. This finding is highly relevant as the membrane composition of all cells differs, but still within a limited window. Even in a single cell, the composition of the membrane is not homogenous, especially when the cell is polarized with highly different membrane properties in the

different parts. For instance, the apical part of epithelial cells contains much more sphingolipids and cholesterol compared to their basolateral part.[38,61] A direct consequence, according to the results of this article, is that the basolateral part of the membrane would be electroporated with milder conditions (lower voltage). In other words, slight changes in the lipidic membrane composition and the cell orientation must be taken into account for the electroporation protocol. This is currently under investigation in our lab, by using either model membranes whose composition is derived from that of the different parts of polarized cells or epithelial cells (MDCK cells). These properties of a cell explain why electroporation experiments are hard to control, also at the single cell level.

Nevertheless, advantage can also be taken from this effect, by controlling the orientation of the cell during the electroporation process so that the basolateral part and not the apical part of the membrane is porated; thereby, the success rate might be enhanced. Similarly, cancer cells are known to have an altered membrane composition compared to their healthy counterparts. The membranes of malignant cells often contain different amounts of cholesterol, sphingolipids and glycerolipids.[75] A direct consequence is that cancer cells would be electroporated at a different voltage than healthy cells. This knowledge can be used to design specific *in vivo* protocols to treat cancer cells while leaving healthy cells untouched (or *vice versa*).

Electroporation measurements as a novel approach for establishing ternary diagrams

The determination of the membrane response to the application of an electric field is shown here as an alternative technique to establish quickly a phase diagram for ternary lipid mixtures. This technique does not require any additional probe or sophisticated equipment, and it is straightforward to record the lipid phase composition. However, electroporation measurements only provide second order information about the membrane phases, as it is not possible to literally "see" the changes in the membrane, its structure as well as its phase composition. Although a good correlation is shown here between the electroporation results and phase transition boundaries reported in literature, it would still be interesting to couple such electrical measurements to more conventional techniques or to investigate a system already described in the literature using our novel methodology. On other aspects, using microscopy techniques, nanodomains cannot be visualized, whereas they are detectable using spectroscopy techniques.[76] Similarly, it would be interesting to determine the sensitivity of the presently described methodology.

Ternary phase diagrams are currently determined using a combination of various techniques. This combined approach is labor-intensive and time-consuming, requiring several years of study before a diagram is fully determined. Interestingly, the approach proposed here lends itself well to multiplexing, especially when combined with microfluidics in lab-on-a-chip devices,[77–79] a field in which our group has much experience.[80,81] By using integrated microfluidic systems containing a series of independently addressed BLMs, the determination of the threshold voltage could be performed on different mixtures simultaneously. Such a microfluidic device would consist of a quick screening tool for the phase domains, after which the interesting regions could be explored in more detail. Furthermore, the time and manual labor could be further reduced by using automated membrane preparation and experimentation techniques.[78,79] These microfluidic devices are already under development, but their interest has till now been limited to pharmaceutical applications for high-throughput screening assays of drugs on membrane proteins.[78,79]

Although complex systems were studied in this paper, these remain simplified models of the cell membrane whose lipid matrix contains over 100 different types of molecules. Besides this, 50% weight of the membranes corresponds to proteins. We have shown here that mixtures of PC, SM and cholesterol give better models of cell membranes. However, two other main components of a cell membrane, glycolipids and proteins, are still missing. In further studies these should be included and their effect investigated.

Abbreviations

BLM	bilayer lipid membrane
Ch	cholesterol
DPhPC	1,2-diphytanoyl-*sn*-glycero-3-phosphocholine
DOPC	dioleoylphosphatidylcholine
L-α-PC	L-α-phosphatidylcholine (Heart, Bovine), a mixture of whose predominant species is 16:0/18:2 PC
l_d	liquid disordered
l_o	liquid ordered
PC	phosphatidylcholine
POPC	palmitoyloleoylphosphatidylcholine
PL	phospholipid
SM	sphingomyelin (Egg, Chicken), a mixture of whose predominant species is 16:0 SM
s_o	solid ordered
V_{th}	threshold voltage for electroporation

Acknowledgements

The authors would like to thank Professor Manuel Prieto from the Centro Química-Física Molecular (Lisbon, Portugal) for critically reading the manuscript and for his useful comments. This work is supported by the Physics of Fluids group from the University of Twente.

References

1 E. Neumann, M. Schaeferridder, Y. Wang and P. H. Hofschneider, *EMBO J.*, 1982, **1**, 841–845.
2 *Electroporation and Electrofusion in Cell Biology*, ed. E. Neumann, A. E. Sowers and C. A. Jordan, Plenum Press, New York, USA, 1989.
3 J. C. Weaver and Y. A. Chizmadzhev, *Bioelectrochem. Bioenerg.*, 1996, **41**, 135–160.
4 *Guide to Electroporation and Electrofusion*, ed. D. C. Chang, B. M. Chassy, J. A. Saunders and A. E. Sowers, Academic Press, Inc., San Diego, CA, USA, 1992.
5 M. B. Fox, D. C. Esveld, A. Valero, R. Luttge, H. C. Mastwijk, P. V. Bartels, A. van den Berg and R. M. Boom, *Anal. Bioanal. Chem.*, 2006, **385**, 474–485.

6 C. Chen, S. W. Smye, M. P. Robinson and J. A. Evans, *Med. Biol. Eng. Comput.*, 2006, **44**, 5–14.
7 M. Golzio, J. Teissie and M. P. Rols, *Bioelectrochemistry*, 2001, **53**, 25–34.
8 A. Valero, J. N. Post, J. W. van Nieuwkasteele, P. M. ter Braak, W. Kruijer and A. van den Berg, *Lab Chip*, 2008, **8**, 62–67.
9 C. Chen, J. A. Evans, M. P. Robinson, S. W. Smye and P. O'Toole, *Phys. Med. Biol.*, 2008, **53**, 4747–4757.
10 L. V. Chernomordik, S. I. Sukharev, S. V. Popov, V. F. Pastushenko, A. V. Sokirko, I. G. Abidor and Y. A. Chizmadzhev, *Biochim. Biophys. Acta*, 1987, **902**, 360–373.
11 M. Hibino, H. Itoh and K. Kinosita, *Biophys. J.*, 1993, **64**, 1789–1800.
12 J. C. Weaver, *IEEE Trans. Dielectr. Electr. Insul.*, 2003, **10**, 754–768.
13 R. A. Bockmann, B. L. de Groot, S. Kakorin, E. Neumann and H. Grubmuller, *Biophys. J.*, 2008, **95**, 1837–1850.
14 S. Koronkiewicz, S. Kalinowski and K. Bryl, *Biochim. Biophys. Acta*, 2002, **1561**, 222–229.
15 W. Krassowska and P. D. Filev, *Biophys. J.*, 2007, **92**, 404–417.
16 K. C. Melikov, V. A. Frolov, A. Shcherbakov, A. V. Samsonov, Y. A. Chizmadzhev and L. V. Chernomordik, *Biophys. J.*, 2001, **80**, 1829–1836.
17 D. P. Tieleman, *BMC Biochem.*, 2004, **5**, 10.
18 M. Winterhalter, *Colloids Surf., A*, 1999, **149**, 161–169.
19 S. J. Marrink, A. H. de Vries and D. P. Tieleman, *Biochim. Biophys. Acta*, 2009, **1788**, 149–168.
20 M. J. Ziegler and P. T. Vernier, *J. Phys. Chem. B*, 2008, **112**, 13588–13596.
21 P. Shil, S. Bidaye and P. B. Vidyasagar, *J. Phys. D: Appl. Phys.*, 2008, **41**, 055502.
22 P. T. Vernier, Z. A. Levine, Y. H. Wu, V. Joubert, M. J. Ziegler, L. M. Mir and D. P. Tieleman, *PloS One*, 2009, **4**, e7966.
23 P. T. Vernier, M. J. Ziegler, Y. H. Sun, W. V. Chang, M. A. Gundersen and D. P. Tieleman, *J. Am. Chem. Soc.*, 2006, **128**, 6288–6289.
24 M. Kanduser, M. Sentjurc and D. Miklavcic, *Eur. Biophys. J.*, 2006, **35**, 196–204.
25 P. F. F. Almeida, *Biochim. Biophys. Acta*, 2009, **1788**, 72–85.
26 M. L. Berkowitz, *Biochim. Biophys. Acta*, 2009, **1788**, 86–96.
27 S. Kakorin, U. Brinkmann and E. Neumann, *Biophys. Chem.*, 2005, **117**, 155–171.
28 S. Koronkiewicz and S. Kalinowski, *Biochim. Biophys. Acta*, 2004, **1661**, 196–203.
29 M. Kotulska, S. Koronkiewicz and S. Kalinowski, *Acta Phys. Pol., B*, 2002, **33**, 1115–1129.
30 T. Rog, M. Pasenkiewicz-Gierula, I. Vattulainen and M. Karttunen, *Biochim. Biophys. Acta*, 2009, **1788**, 97–121.
31 I. van Uitert, S. Le Gac and A. van den Berg, *Biochim. Biophys. Acta*, 2010, **1798**, 21–31.
32 S. W. I. Siu and R. A. Bockmann, *J. Struct. Biol.*, 2007, **157**, 545–556.
33 M. Tarek, *Biophys. J.*, 2005, **88**, 4045–4053.
34 G. C. Troiano, K. J. Stebe, R. M. Raphael and L. Tung, *Biophys. J.*, 1999, **76**, 3150–3157.
35 K. Jacobson, E. D. Sheets and R. Simson, *Science*, 1995, **268**, 1441–1442.
36 S. J. Singer and G. L. Nicolson, *Science*, 1972, **175**, 720.
37 T. Heimburg, *Thermal Biophysics of Membranes*, WILEY-VCH Verlag GmbH, Wienheim, 1st edn, 2007.
38 K. Simons and W. L. C. Vaz, *Annu. Rev. Biophys. Biomol. Struct.*, 2004, **33**, 269–295.
39 B. Ramstedt and J. P. Slotte, *Biochim. Biophys. Acta*, 2006, **1758**, 1945–1956.
40 D. A. Brown and E. London, *J. Biol. Chem.*, 2000, **275**, 17221–17224.
41 J. R. Silvius, *Biochim. Biophys. Acta*, 2003, **1610**, 174–183.
42 P. R. Cullis and B. Dekruijff, *Biochim. Biophys. Acta*, 1979, **559**, 399–420.
43 J. N. Israelachvili and D. J. Mitchell, *Biochim. Biophys. Acta*, 1975, **389**, 13–19.
44 J. M. Smaby, H. L. Brockman and R. E. Brown, *Biochemistry*, 1994, **33**, 9135–9142.
45 S. L. Veatch and S. L. Keller, *Phys. Rev. Lett.*, 2005, **94**, 148101.
46 T. Y. Wang and J. R. Silvius, *Biophys. J.*, 2000, **79**, 1478–1489.
47 L. J. Pike, *J. Lipid Res.*, 2006, **47**, 1597–1598.
48 S. Semrau and T. Schmidt, *Soft Matter*, 2009, **5**, 3174–3186.
49 M. D. Collins and S. L. Keller, *Proc. Natl. Acad. Sci. U. S. A.*, 2008, **105**, 124–128.
50 S. L. Veatch and S. L. Keller, *Biophys. J.*, 2003, **85**, 3074–3083.
51 B. Alberts, D. Bray, J. Lewis, M. Raff, K. Roberts and J. D. Watson, *Molecular Biology of the Cell*, Garland Publishing, Inc., New York, NY, USA, 2nd edn, 1989.
52 H. Ohvo-Rekila, B. Ramstedt, P. Leppimaki and J. P. Slotte, *Prog. Lipid Res.*, 2002, **41**, 66–97.
53 P. Mueller, W. C. Wescott, D. O. Rudin and H. T. Tien, *J. Phys. Chem.*, 1963, **67**, 534.
54 A. Wiese and U. Seydel, in *Methods in Molecular Biology*, ed. O. Holst, Humana Press Inc., Totowa, NJ, 2000, pp. 355–370.
55 R. F. M. de Almeida, A. Fedorov and M. Prieto, *Biophys. J.*, 2003, **85**, 2406–2416.
56 *Lipid Thermotropic Phase Transition Database*, 1997, http://www.lipidat.ul.ie.
57 B. Dekruijff, P. R. Cullis and G. K. Radda, *Biochim. Biophys. Acta*, 1976, **436**, 729–740.
58 S. W. Hui and A. Sen, *Proc. Natl. Acad. Sci. U. S. A.*, 1989, **86**, 5825–5829.
59 E. Karatekin, O. Sandre, H. Guitouni, N. Borghi, P. H. Puech and F. Brochard-Wyart, *Biophys. J.*, 2003, **84**, 1734–1749.
60 J. Y. Huang and G. W. Feigenson, *Biophys. J.*, 1999, **76**, 2142–2157.
61 D. Marsh, *Biochim. Biophys. Acta*, 2009, **1788**, 2114–2123.
62 J. Y. Huang, J. T. Buboltz and G. W. Feigenson, *Biochim. Biophys. Acta*, 1999, **1417**, 89–100.
63 N. Kahya, D. Scherfeld, K. Bacia, B. Poolman and P. Schwille, *J. Biol. Chem.*, 2003, **278**, 28109–28115.
64 A. Pokorny, L. E. Yandek, A. I. Elegbede, A. Hinderliter and P. F. F. Almeida, *Biophys. J.*, 2006, **91**, 2184–2197.
65 G. W. Feigenson, *Nat. Chem. Biol.*, 2006, **2**, 560–563.
66 G. W. Feigenson, *Biochim. Biophys. Acta*, 2009, **1788**, 47–52.
67 J. L. Thewalt and M. Bloom, *Biophys. J.*, 1992, **63**, 1176–1181.
68 S. L. Veatch, I. V. Polozov, K. Gawrisch and S. L. Keller, *Biophys. J.*, 2004, **86**, 2910–2922.
69 M. R. Vist and J. H. Davis, *Biochemistry*, 1990, **29**, 451–464.
70 M. I. Collado, F. M. Goni, A. Alonso and D. Marsh, *Biochemistry*, 2005, **44**, 4911–4918.
71 G. W. Feigenson and J. T. Buboltz, *Biophys. J.*, 2001, **80**, 2775–2788.
72 P. E. Milhiet, C. Domec, M. C. Giocondi, N. Van Mau, F. Heitz and C. Le Grimellec, *Biophys. J.*, 2001, **81**, 547–555.
73 P. E. Milhiet, M. C. Giocondi and C. Le Grimellec, *J. Biol. Chem.*, 2002, **277**, 875–878.
74 C. B. Yuan and L. J. Johnston, *Biophys. J.*, 2001, **81**, 1059–1069.
75 A. B. Hendrich and K. Michalak, *Curr. Drug Targets*, 2003, **4**, 23–30.
76 F. M. Goni, A. Alonso, L. A. Bagatolli, R. E. Brown, D. Marsh, M. Prieto and J. L. Thewalt, *Biochim. Biophys. Acta*, 2008, **1781**, 665–684.
77 B. Le Pioufle, H. Suzuki, K. V. Tabata, H. Noji and S. Takeuchi, *Anal. Chem.*, 2008, **80**, 328–332.
78 H. Suzuki, B. Le Pioufle and S. Takeuhci, *Biomed. Microdevices*, 2009, **11**, 17–22.
79 M. Zagnoni, M. E. Sandison and H. Morgan, *Biosens. Bioelectron.*, 2009, **24**, 1235–1240.
80 H. Andersson and A. van den Berg, *Sens. Actuators, B*, 2003, **92**, 315–325.
81 S. Le Gac and A. van den Berg, *Trends Biotechnol.*, 2010, **28**, 55–62.